DAMPED Lyα ABSORPTION ASSOCIATED WITH AN EARLY-TYPE GALAXY AT REDSHIFT $z = 0.16377$[1,2]

KENNETH M. LANZETTA[3], ARTHUR M. WOLFE[4], HAKAN ALTAN[3], XAVIER BARCONS[5,6], HSIAO-WEN CHEN[3], ALBERTO FERNÁNDEZ-SOTO[3], DAVID M. MEYER[7], AMELIA ORTIZ-GIL[3], SANDRA SAVAGLIO[8], JOHN K. WEBB[9], and NORIAKI YAHATA[3]

[1]Based on observations with the NASA/ESA Hubble Space Telescope, obtained at the Space Telescope Science Institute, which is operated by the Association of Universities for Research in Astronomy, Inc., under NASA contract NAS5–26555.

[2]Based on observations made with the William Herschel Telescope operated on the island of La Palma by the Royal Greenwich Observatory in the Spanish Observatorio del Roque de Los Muchachos of the Instituto de Astrofísica de Canarias.

[3]Astronomy Program, Department of Earth and Space Sciences, State University of New York at Stony Brook, Stony Brook, NY 11794–2100, U.S.A.

[4]Center for Astrophysics and Space Sciences, University of California, San Diego, La Jolla, CA 92093–0111, U.S.A.

[5]Instituto de Física de Cantabria (Consejo Superior de Investigaciones Científicas—Universidad de Cantabria), Facultad de Ciencias, 39005 Santander, SPAIN

[6]Institute of Astronomy, Madingley Road, Cambridge CB3 0HA, ENGLAND

[7]Department of Physics and Astronomy, Northwestern University, Evanston, IL 60208, U.S.A.

[8]European Southern Observatory, K. Schwarzschild Str. 2, Garching b. München, D–85748, GERMANY

[9]School of Physics, University of New South Wales, P.O. Box 1, Kensington, NSW 2033, AUSTRALIA

ABSTRACT

We report new HST and ground-based observations of a damped Lyα absorption system toward the QSO 0850+4400. The redshift of the absorption system is $z = 0.163770 \pm 0.000054$ and the neutral hydrogen column density of the absorption system is $\log N = 19.81 \pm 0.04$ cm^{-2}. The absorption system is by far the lowest redshift confirmed damped Lyα absorption system yet identified, which provides an unprecedented opportunity to examine the nature, impact geometry, and kinematics of the absorbing galaxy in great detail. The observations indicate that the absorption system is remarkable in three respects: First, the absorption system is characterized by weak metal absorption lines and a low metal abundance, possibly less than 4% of the solar metal abundance. This cannot be explained as a consequence of obscuration by dust, because the neutral hydrogen column density of the absorption system is far too low for obscuration by dust to introduce any significant selection effects. Second, the absorption system is associated with a moderate-luminosity early-type S0 galaxy, although the absorption may actually arise in one of several very faint galaxies detected very close to the QSO line of sight. Third, the absorbing material moves counter to the rotating galaxy disk, which rules out the possibility that the absorption arises in a thin or thick co-rotating gaseous disk. These results run contrary to the expectation that low-redshift damped Lyα absorption systems generally arise in the gas- and metal-rich inner parts of late-type spiral galaxies. We suggest instead that mounting evidence indicates that low-redshift galaxies of a variety of morphological types may contain significant quantities of low metal abundance gas at large galactocentric distances.

Subject headings: galaxies: evolution—quasars: absorption lines

1. INTRODUCTION

Damped Lyα absorption systems detected toward background QSOs trace the gaseous content of the universe to very high redshifts. Most surveys for damped Lyα absorption systems have been carried out at optical wavelengths (Wolfe et al. 1986; Lanzetta et al. 1991; Wolfe et al. 1995; Storrie-Lombardi, Irwin, & McMahon 1996), where the absorbers are detected at redshifts ranging from $z \approx 1.6$ (the redshift of Lyα at the atmospheric cutoff) through $z \approx 5$ (the redshift of the most distant background QSOs in the surveys). These optical surveys have demonstrated that damped Lyα absorption systems dominate the mass density of neutral gas in the universe, containing roughly enough gas at $z \approx 3.5$ to form the stars of present-day galaxies. But although the redshifts sampled by the optical surveys span an important epoch in the history of galaxy evolution, the cosmic time interval spanned by the optical surveys corresponds to only a small fraction of the current age of the universe.

To address this issue, we are conducting a spectroscopic survey of damped Lyα absorption systems at ultraviolet wavelengths, based on archival International Ultraviolet Explorer (IUE) and Hubble Space Telescope (HST) low-resolution spectroscopy and targeted HST high-resolution spectroscopy (Lanzetta, Wolfe, & Turnshek 1995; Lanzetta et al. in preparation). A primary goal of the survey is to identify damped Lyα absorption systems at very low redshifts, in order both to measure the gaseous content of the nearby universe and to secure a sample of nearby absorbers for detailed study. We have so far surveyed ultraviolet spectra of more than 500 QSOs, BL Lac objects, and Seyfert galaxies, and we have obtained confirming (or otherwise) spectra of most of the candidate damped Lyα absorption systems identified in low-resolution or low signal-to-noise ratio observations.

Full results of the survey will be presented elsewhere, but here we report new HST and ground-based observations of a damped Lyα absorption system identified in the survey at redshift $z = 0.16377$ toward the QSO 0850+4400. The absorption system is of particular interest because it was identified not only in our spectroscopic survey of damped Lyα absorption systems but also in our imaging and spectroscopic survey of galaxies and absorption systems toward HST spectroscopic target QSOs (Lanzetta et al. 1995), in which it was found to be associated with a galaxy just 16.6 h^{-1} kpc from the QSO line of sight. The absorption system is by far the lowest redshift confirmed damped Lyα absorption system yet identified, which provides an unprecedented opportunity to examine the nature, impact geometry, and kinematics of the absorbing galaxy in great detail.

The HST observations reported here include (1) a new Goddard High Resolution Spectrograph (GHRS) spectrum of 0850+4400 and (2) a new Wide Field Planetary Camera 2 (WFPC2) image of the field surrounding 0850+4400. The ground-based observations reported here include (3) a new spectrum of the galaxy associated with the absorption system. A dimensionless Hubble constant $h = H_0/(100 \text{ km s}^{-1} \text{ Mpc}^{-1})$ and a deceleration parameter $q_0 = 0.5$ are adopted throughout.

2. OBSERVATIONS

2.1. GHRS Spectroscopy

Spectroscopic observations of 0850+4400 were obtained with HST using GHRS with the G140L grating on 28 September 1996. The observations were obtained in a series of 16 exposures each of 300 s duration for a total exposure time of 4800 s. The individual exposures were reduced using standard pipeline techniques and were registered to a common origin and coadded using our own reduction programs. The final spectrum was fitted with a smooth continuum using an iterative spline fitting technique. The spectral resolution of the final spectrum was measured to be FWHM = 0.60 Å, and the continuum signal-to-noise ratio of the final spectrum was measured to be $S/N \approx 12$ per resolution element. A portion of the spectrum is shown in Figure 1.

2.2. WFPC2 Imaging

Imaging observations of objects in the field surrounding 0850+4400 were obtained with HST using WFPC2 with the F702W filter on 7 February 1996. The observations were obtained in a series of three exposures each of 800 s duration for a total exposure time of 2400 s. The individual exposures were reduced using standard pipeline techniques and were registered to a common origin, filtered for cosmic rays, and coadded using our own reduction programs. The spatial resolution of the final image was measured to be FWHM $\approx$ 0.1 arcsec, and the 5σ detection threshold of the final image to point sources was measured to be $AB(7020) = 26.3$. A portion of the image is shown in Figure 2.

2.3. WHT Spectroscopy

Spectroscopic observations of galaxy −00089+00020 were obtained with the William Herschel Telescope (WHT) using the ISIS double spectrograph with two 1200 line mm^{-1} gratings and two Tektronix CCD detectors on 4 March 1995. (Here and throughout galaxies are indicated by noting their coordinate offsets in Right Ascension and Declination, respectively, from the QSO line of sight in units of 0.1 arcsec.) The observations were obtained in a series of three exposures each of 1800 s duration for a total exposure time of 5400 s. A long slit of width 1.5 arcsec was aligned to a position angle of 50 deg, which is roughly coincident with the major axis of the galaxy. Observations of a Cu-Ar and a Cu-Ne arc lamp were obtained following each exposure, and observations of a tungsten lamp were obtained at the end of the night. The individual exposures were bias subtracted, flatfielded, and extracted using our own reduction programs, and the resulting spectra were wavelength calibrated by means of fifth-order polynomial fits to spectral lines identified in the arc lamp observations. The RMS residuals of the polynomial fits were measured to be 0.03 Å (of the blue spectrum) and 0.05 Å (of the red spectrum). The wavelength scales were reduced

to vacuum, heliocentric values. The spectral resolutions of the final spectra were measured to be FWHM = 1.14 Å (of the blue spectrum) and FWHM = 1.07 Å (of the red spectrum).

2.4. Other Observations

In addition to the new observations described above, other observations are relevant to the present analysis: First, we obtained imaging and spectroscopic observations of 16 faint galaxies and stars (including galaxy −00089+00020) in the field surrounding 0850+4400 (Lanzetta et al. 1995; Lanzetta et al. in preparation). Second, Bahcall et al. (1995) obtained Faint Object Spectrograph (FOS) G160L, G190H, and G270H spectra of 0850+4400, which we accessed through the HST archive. These other observations will be considered as appropriate in the analysis described below.

3. ANALYSIS

3.1. Absorption System Spectroscopy

In this section we consider the GHRS G140L spectrum described in § 2.1 and the FOS G190H and G270H spectra mentioned in § 2.4 in order to (1) measure physical parameters of the absorption system and (2) characterize the metal content of the absorption system.

To measure physical parameters of the absorption system, we applied the χ^2 Voigt profile fitting routine described by Lanzetta & Bowen (1992) to the GHRS G140L spectrum, adopting the redshift, Doppler parameter, and neutral hydrogen column density as parameters. The resulting fit is shown in Figure 1. The redshift of the absorption system is

$$z = 0.163770 \pm 0.000054 \tag{1}$$

and the neutral hydrogen column density of the absorption system is

$$\log N = 19.81 \pm 0.04 \text{ cm}^{-2}, \tag{2}$$

which corresponds to a rest-frame equivalent width of

$$W = 5.9 \pm 0.3 \text{ Å}. \tag{3}$$

The Doppler parameter of the absorption system is essentially unconstrained because the absorption line occurs on the damped part of the curve of growth. To determine whether the total column density estimate could be affected by unresolved velocity structure, we repeated the analysis allowing for two absorbing components. We found that it is not possible to obtain a fit with a significantly lower total column density. Regardless of how the initial parameter values were set, the final solution always converged to a total column density consistent with the value of equation (2) to within formal uncertainties.

To characterize the metal content of the absorption system, we searched for prominent metal absorption lines at the redshift of the absorption system in the GHRS G140L and FOS G190H and G270H spectra. The GHRS G140L spectrum covers predicted absorption lines of N V, O I, Si II, and S II; the FOS G190H spectrum covers predicted absorption lines of C IV and Si IV; and the FOS G270H spectrum covers predicted absorption lines of Mg II, Mn II, and Fe II. The resulting measurements or upper limits are given in Table 1. Of 26 predicted absorption lines covered by the spectra, absorption lines are tentatively detected only at the predicted wavelengths of C IV λ1548, Mg II λ2803, Si II λ1193, and Si II λ1260. But no absorption lines are detected at the predicted wavelengths of corresponding C IV λ1550, Mg II λ2796, Si II λ1190, or Si II λ1304, suggesting that the detected absorption lines might be unrelated chance coincidences. The most stringent limit to the metal abundance of the absorption system is set by the absence of detectable O I λ1302 absorption, because O^0 has an ionization potential very nearly equal to one Rydberg and O^0/H^0 is expected to trace O/H under a variety of ionization conditions. But the upper limit to the O^0 column density depends sensitively on the Doppler parameter, which is unknown. We therefore calculated the column densities corresponding to the O I λ1302 equivalent width limit of Table 1 for assumed Doppler parameters of 30, 10, 5, and 2 km s^{-1}. The resulting upper limits are given in Table 2. For any Doppler parameter satisfying $b > 10$ km s^{-1}, the 2σ upper limit to the O^0 column density satisfies $\log N < 15.39$ cm^{-2}, which adopting the neutral hydrogen column density of equation (2) corresponds to a 2σ upper limit to the O abundance of [O/H] < -1.36, or less than 4% of the solar metal abundance. The O abundance could be appreciably higher than this only if the Doppler parameter is less than 10 km s^{-1}, which cannot be ruled out by the present observations.

3.2. Galaxy Imaging

In this section we consider the WFPC2 F702W image described in § 2.2 and the imaging and spectroscopic observations of faint galaxies and stars mentioned in § 2.4 in order to (1) measure morphological and spectral parameters of the galaxy and (2) search for faint galaxies very close to the QSO line of sight.

The absorption system is associated with galaxy −00089+00020, which the imaging and spectroscopic observations of Lanzetta et al. (1995) indicate occurs at redshift $z \approx 0.1634$ and impact parameter $\rho = 16.6\ h^{-1}$ kpc. These observations spectroscopically identify a total of 16 faint galaxies and stars in the field but no other galaxies at redshift $z \approx 0.16$.

To measure morphological parameters of the galaxy, we applied the χ^2 disk plus bulge profile fitting routine described by Chen et al. (1997) to the WFPC2 F702W image, adopting the position, disk and bulge effective (or half-light) surface brightnesses, disk and bulge effective (or half-light) radii, inclination angle and axis ratio, and orientation angle as parameters. The disk effective radius of the galaxy is

$$R_D = 1.4 \pm 0.3\ h^{-1}\ \text{kpc}, \tag{4}$$

and the bulge effective radius of the galaxy is

$$R_B = 2.5 \pm 0.2\ h^{-1}\ \mathrm{kpc}. \tag{5}$$

The disk inclination angle of the galaxy is

$$i = 50 \pm 2\ \mathrm{deg}, \tag{6}$$

and the position angle of the major axis of the galaxy is

$$\mathrm{PA} = 52 \pm 2\ \mathrm{deg}, \tag{7}$$

which forms an angle to the projected line segment joining the galaxy to the QSO of

$$\alpha = 51 \pm 2\ \mathrm{deg}. \tag{8}$$

Directly integrating the theoretical surface brightness profiles, the integrated disk-to-bulge ratio of the galaxy is

$$D/B = 0.4 \pm 0.1, \tag{9}$$

and the apparent magnitude of the galaxy is

$$AB(7020) = 19.21 \pm 0.01. \tag{10}$$

To measure spectral parameters of the galaxy, we applied the galaxy spectral classification routine described by Yahata et al. (in preparation) to the spectrum of galaxy −00089+00020 of Lanzetta et al. (1995). The galaxy is spectrally classified as an Sb galaxy, and the rest-frame B-band absolute magnitude of the galaxy (applying an appropriate K correction calculated from the spectral energy distributions of Coleman, Wu, & Weedman 1980) is

$$M_B - 5\log h = -18.61 \pm 0.01. \tag{11}$$

Taking the rest-frame B-band absolute magnitude of an L_* galaxy to be $M_{B_*} - 5\log h = -19.5$, this corresponds to rest-frame B-band luminosity of

$$L_B = 0.4 L_{B_*}. \tag{12}$$

To search for faint galaxies very close to the QSO line of sight, we subtracted a Tiny Tim (Krist 1995) point spread function model of the QSO from the WFPC2 F702W image. The resulting image is shown in Figure 3. The image reveals several very faint galaxies very close to the QSO line of sight, for which spectroscopic identifications have not yet been obtained. Galaxy +00004+00019 is of angular separation 1.9 arcsec and apparent magnitude $AB(7020) = 22.5$, galaxy −00026+00024 is of angular separation 3.5 arcsec and apparent magnitude $AB(7020) = 24.5$, and galaxy −00023+00043 is of angular separation 4.9 arcsec and apparent magnitude $AB(7020) = 26.1$. If these galaxies are at the redshift of the absorption system, then they occur at impact parameters ranging from $\rho = 3.8\ h^{-1}$ kpc (galaxy +00004+00019) to $\rho = 8.7\ h^{-1}$ kpc (galaxy −00023+00043) and rest-frame B-band luminosities (applying the K correction calculated for galaxy −00089+00020) ranging from $L_B = 0.002 L_{B_*}$ (galaxy −00023+00043) to $L_B = 0.05 L_{B_*}$ (galaxy +00004+00019). Alternatively, the galaxies might occur at the redshift $z = 0.513$ of the QSO, in which case they are not related to the absorption system.

3.3. Galaxy Spectroscopy

In this section we consider the WHT ISIS spectrum described in § 2.3 in order to (1) measure spectral properties of galaxy −00089+00020 and (2) compare the rotation curve of the galaxy with the velocity of the absorption system.

To measure spectral properties of the galaxy, we obtained Gaussian fits to the Hα and [N II] emission lines of the WHT ISIS spectrum, adopting the systemic redshift, velocity width, and peak intensity as parameters. The systemic redshift of the galaxy is

$$z = 0.163483 \pm 0.000011, \tag{13}$$

which adopting the redshift of the absorption system of equation (1) corresponds to a velocity difference between the galaxy and the absorption system of

$$74 \pm 14 \text{ km s}^{-1}. \tag{14}$$

To compare the rotation curve of the galaxy with the velocity of the absorption system, we extracted a spatially- and spectrally-resolved image of the Hα emission line of the WHT ISIS spectrum. Following Barcons, Lanzetta, & Webb (1995), we corrected the projected velocity v and impact parameter ρ to the line joining the center of the galaxy to the QSO line of sight by assuming circular motion of a flat disk. The resulting rotation curve together with a point indicating the velocity and impact parameter difference between the galaxy and the absorption system is shown in Figure 4. The absorbing material does not participate in the rotation of the galaxy disk. Rather the absorbing material moves counter to the rotating galaxy disk, missing the predicted motion of the galaxy disk by more than 150 km s^{-1} at an impact parameter of 16.6 h^{-1} kpc. This observation rules out the possibility that the absorbing material arises in a thin or thick co-rotating gaseous disk.

3.4. Nature of Galaxy −00089+00020

Considering the visual appearance, size, integrated disk-to-bulge ratio, and rest-frame B-band luminosity, we conclude that galaxy −00089+00020 is a moderate luminosity early-type S0 galaxy.

4. SUMMARY AND DISCUSSION

The main results of the analysis are summarized as follows:

1. The damped Lyα absorption system toward 0850+4400 identified in our spectroscopic survey of damped Lyα absorption systems at ultraviolet wavelengths (Lanzetta, Wolfe, & Turnshek 1995; Lanzetta et al. in preparation) and in our imaging and spectroscopic survey of galaxies and

absorption systems toward HST spectroscopic target QSOs (Lanzetta et al. 1995) is confirmed by a GHRS G140L spectrum. The redshift of the absorption system is $z = 0.163770 \pm 0.000054$ and the neutral hydrogen column density of the absorption system is $\log N = 19.81 \pm 0.04$ cm^{-2}. The absorption system is by far the lowest redshift confirmed damped Lyα absorption system yet identified, which provides an unprecedented opportunity to examine the nature, impact geometry, and kinematics of the absorbing galaxy in great detail.

2. The absorption system is characterized by weak metal absorption lines and low metal abundances. No absorption lines of N V, O I, Si IV, S II, Mn II, or Fe II are detected to within sensitive upper limits, although weak absorption lines of C IV, Mg II, and Si II may be present. The most stringent limit to the metal abundance of the absorption system is set by the absence of detectable O I absorption, which places a 2σ upper limit to the O abundance of [O/H] < -1.36 (or less than 4% of the solar O abundance) if the Doppler parameter of the absorption system satisfies $b > 10$ km s^{-1} (although a smaller Doppler parameter and a correspondingly larger O abundance cannot be ruled out by the present observations).

3. The absorption system is associated with a moderate-luminosity early-type S0 galaxy. The the impact parameter of the galaxy is $\rho = 16.6\ h^{-1}$ kpc and the rest-frame B-band luminosity of the galaxy is $L_B = 0.4 L_{B_*}$. No other galaxies in the field are identified at a comparable redshift, and no other galaxies of luminosity exceeding $L_B = 0.05 L_{B_*}$ are present at smaller impact parameters. The absorption may actually arise in one of several very faint galaxies detected very close to the QSO line of sight for which spectroscopic identifications have not yet been obtained.

4. The redshift of the galaxy is $z = 0.163483 \pm 0.000011$, and the velocity difference between the galaxy and the absorption system is 74 ± 14 km s^{-1}. The absorbing material moves counter to the rotating galaxy disk, which rules out the possibility that the absorption arises in a thin or thick co-rotating disk.

Our first conclusion is that these results run contrary to the expectation that low-redshift damped Lyα absorption systems generally arise in the gas- and metal-rich inner parts of late-type spiral galaxies, which are thought to dominate the gaseous content of the nearby universe (Rao & Briggs 1993). Instead these results fit a pattern that appears to be emerging from observations of several other damped Lyα absorption systems at redshifts $z < 1.6$. Specifically, a number of recent observations indicate that low-redshift damped Lyα absorption systems very often (1) exhibit low metal abundances (with evidence of Population II metal abundance patterns) (Meyer & York 1992; Steidel et al. 1995; Meyer, Lanzetta, & Wolfe 1995) and (2) arise far from the inner regions of galaxies of a variety of morphological types (Steidel et al. 1997; Le Brun et al. 1997). In contrast, there are *no* known examples of low-redshift damped Lyα absorption systems that exhibit solar or near-solar metal abundances and only one known example of a low-redshift damped Lyα absorption system that arises in the inner region of late-type spiral galaxy (Le Brun et al. 1997). Why is it that apparently "anomalous" observations appear to be the rule rather than the exception?

Previous authors have argued that obscuration by dust might preferentially favor selection of

chemically unevolved galaxies of lower dust content over chemically evolved galaxies of higher dust content (e.g. Steidel et al. 1994; Pei & Fall 1995; Steidel et al. 1997). But it is easy to show that the neutral hydrogen column density of the absorption system toward 0850+4400 is far too low for obscuration by dust to introduce any significant selection effects. Even adopting a Galactic dust-to-gas ratio and dust extinction curve, the predicted V-band extinction caused by the absorption system amounts to no more than 0.05 mag. Yet the V-band magnitude of 0850+4400 is $V = 16.62$, which is almost 1.5 mag brighter than the nominal magnitude limit $V \approx 18$ of the HST survey for damped Lyα absorption systems. Hence the absorption system would have been included into the survey essentially irrespective of dust content, and the observations *cannot* be explained as a consequence of obscuration by dust. Similar arguments indicate that obscuration by dust is also unlikely to explain the observations of the other low-redshift damped Lyα absorption systems, which are also generally characterized by low neutral hydrogen column densities (c.f. Meyer, Lanzetta, & Wolfe 1995).

We suggest instead that mounting evidence indicates that the observations must be taken seriously as indicative of the gaseous content of the low-redshift universe. Because damped Lyα absorption systems dominate the mass density of neutral gas in the low-redshift universe (Lanzetta, Wolfe, & Turnshek 1995), a straightforward interpretation is that the observations indicate that galaxies of a variety of morphological types may contain significant quantities of low metal abundance gas at large galactocentric distances. This gas could constitute roughly half of the mass density of neutral gas in the low-redshift universe, based on the very limited statistics that are so far available. The existence of such gas can in principle be confirmed by means of additional observations of low-redshift damped Lyα absorption systems.

Our second conclusion is that these results run contrary to the hypothesis that damped Lyα absorption systems arise in rotating ensembles of clouds (Lanzetta & Bowen 1992; Prochaska & Wolfe 1997). This hypothesis was advanced to explain the observation that metal absorption lines of damped Lyα absorption systems very often exhibit asymmetric absorption profiles that are characteristic of rotational motion. Of course, in this case no significant metal absorption lines are detected, so it is not possible to tell whether the absorption system does or does not exhibit this signature. The asymmetric absorption profiles have been previously identified only in connection with higher column density absorbing material (i.e. with neutral hydrogen column densities satisfying $\log N > 20.3$ cm^{-2}), hence it is possible that higher column density absorption systems arise in rotating ensemble of clouds and lower column density absorption systems do not. Similar observations of other low-redshift galaxy and absorption system pairs are needed to establish the relationship between the stellar and gaseous kinematics of galaxies.

The observations reported here have two other notable implications as follows:

First, the observation that the absorption system is characterized by weak metal absorption lines (e.g. with no detectable Mg II $\lambda\lambda 2796, 2803$ doublet) demonstrates that low-redshift damped Lyα absorption systems cannot be reliably identified on the basis of metal absorption lines. Previous

attempts to identify low-redshift damped Lyα absorption systems from known Mg II absorption systems (e.g. Rao, Turnshek, & Briggs 1995) are apparently biased toward absorption systems with stronger metal absorption lines and higher metal abundances.

Second, the observation of the reality of the absorption system helps to establish the anti-correlation between Lyα absorption equivalent width and galaxy impact parameter found in our previous analysis (Lanzetta et al. 1995). Subsequent authors doubted the reality of the absorption system and excluded it from consideration in their analyses, which failed to detect the anti-correlation between Lyα absorption equivalent width and galaxy impact parameter (e.g. Le Brun, Bergeron, & Boisse 1996). The galaxy and absorption system pair toward 0850+4400 (of Lyα absorption equivalent width $W = 5.9$ Å and galaxy impact parameter $\rho = 16.6\ h^{-1}$ kpc) apparently must be included into any objective and unbiased analysis of the relationship between Lyα absorption equivalent width and galaxy impact parameter.

The authors thank the staff of STScI for their expert assistance. H.A., H.-W.C., A.F-S., K.M.L., A.O.-G., and N.Y. were supported by grant NAG–53261 from NASA; grants AR–0580–30194A, GO–0594–80194A, GO–0594–90194A, and GO–0661–20195A from STScI; and grant AST–9624216 from NSF. X.B. was partially supported by the DGES under project PB95–0122 and acknowledges sabbatical support at Cambridge by the DGES under grant PR95—490.

TABLE 1
REST-FRAME EQUIVALENT WIDTHS OF METAL ABSORPTION LINES[a]

Absorption Line	W (Å)	σ_W (Å)
C IV λ1548	0.23	0.06
C IV λ1550	< 0.04	...
N V λ1238	< 0.07	...
N V λ1242	< 0.08	...
O I λ1302	< 0.09	...
Mg II λ2796	< 0.19	...
Mg II λ2803	0.43	0.11
Al II λ1670	< 0.16	...
Si II λ1190	< 0.07	...
Si II λ1193	0.15	0.03
Si II λ1260	0.10	0.03
Si II λ1304	< 0.10	...
Si IV λ1393	< 0.63	...
Si IV λ1402	< 0.44	...
S II λ1250	< 0.08	...
S II λ1253	< 0.08	...
S II λ1259	< 0.07	...
Mn II λ2576	< 0.19	...
Mn II λ2594	< 0.20	...
Mn II λ2606	< 0.20	...
Fe II λ1608	< 0.10	...
Fe II λ2344	< 0.18	...
Fe II λ2374	< 0.19	...
Fe II λ2382	< 0.19	...
Fe II λ2586	< 0.19	...
Fe II λ2600	< 0.19	...

[a]Upper limits are 2σ.

TABLE 2
UPPER LIMITS TO
O^0 COLUMN DENSITY[a]

b (km s^{-1})	$\log N$ (cm^{-2})
30	< 14.56
10	< 15.39
5	< 17.87
2	< 18.17

[a]Upper limits are 2σ.

REFERENCES

Bahcall, J. N., et al. 1993, ApJS, 87, 1

Barcons, X., Lanzetta, K. M., & Webb, J. K. 1995, Nature, 376, 321

Chen, H.-W., Lanzetta, K. M., Webb, J. K., & Barcons, X. 1997, ApJ, submitted

Coleman, G. D., Wu, C. C. & Weedman, D. W. 1980, ApJS, 43, 393

Krist, J. 1995, in Astronomical Data Analysis Software and Systems IV, ASP Conference Series, Vol. 77, ed. R. A. Shaw, H. E. Payne, & J. J. E. Hayes (San Francisco: Astronomical Society of the Pacific), p. 349

Lanzetta, K. M., & Bowen, D. V. 1992, ApJ, 391, 48

Lanzetta, K. M., Bowen, D. V., Tytler, D., & Webb, J. K. 1995, ApJ, 442, 538

Lanzetta, K. M., Wolfe, A. M., & Turnshek, D. A. 1995, ApJ, 440, 435

Lanzetta, K. M., Wolfe, A. M., Turnshek, D. A., Lu, L., McMahon, R. G., & Hazard, C. 1991, ApJS, 77, 1

Le Brun, V., Bergeron, J., & Boisse, P. 1996, A&A, 306, 691

Le Brun, V., Bergeron, J., Boisse, P., & Deharveng, J. M. 1997, A&A, in press

Meyer, D. M., Lanzetta, K. M., & Wolfe, A. M. 1995, ApJ, 399, L121

Meyer, D. M., & York, D. G. 1992, ApJ, 399, L121

Pei, Y. C., & Fall, S. M. 1995, ApJ, 454, 69

Prochaska, J. X., & Wolfe, A. M. 1997, ApJ, in press

Rao, S. M., & Briggs, F. H. 1993, ApJ, 419, 515

Rao, S. M., Turnshek, D. A., & Briggs, F. H. 1995, ApJ, 449, 488

Steidel, C. C., Bowen, D. V., Blades, J. C., & Dickinson, M. 1995, ApJ, 440, L45

Steidel, C. C., Dickinson, M., Meyer, D. M., Adelberger, K. L., & Sembach, K. R. 1997, ApJ, 480, 568

Steidel, C. C., Pettini, M., Dickinson, M., & Persson, S. E. 1994, AJ, 108, 2046

Storrie-Lombardi, L. J., McMahon, R. G., Irwin, M. J., & Hazard, C. 1996, ApJ, 468, 128

Wolfe, A. M., Lanzetta, K. M., Foltz, C. B., & Chaffee, F. 1995, ApJ, 454, 698

Wolfe, A. M., Turnshek, D. A., Smith, H. E., & Cohen, R. D. 1986, ApJS, 61, 249

Fig. 1.— Portion of GHRS G140L spectrum of 0850+4400 centered on Lyα absorption line. Spectral resolution is FWHM = 0.60 Å (or FWHM = 130 km s^{-1}), and continuum signal-to-noise ratio is $S/N \approx 12$ per resolution element. Spectrum has been smoothed at roughly the Nyquist rate. Smooth curve shows χ^2 Voigt profile fit, which indicates a redshift $z = 0.163770 \pm 0.000054$ and a neutral hydrogen column density $\log N = 19.81 \pm 0.04$ cm^{-2}.

Fig. 2.— Portion of WFPC2 F702W image of field surrounding 0850+4400. Spatial resolution is FWHM = 0.1 arcsec, and angular extent is 40×40 arcsec^2. Indicated objects have been spectroscopically identified (Lanzetta et al. 1995; Lanzetta et al. in preparation). Object −00089+00020 is a galaxy of redshift $z = 0.1635$, object +00000+00000 is 0850+4400, object −00001−00050 is a star, object +00100−00024 is a galaxy of redshift $z = 0.4402$, and object +00226+00124 is a galaxy of redshift $z = 0.5007$.

Fig. 3.— Portion of WFPC2 F702W image of field surrounding 0850+4400 for which a Tiny Tim point spread function model of the QSO has been subtracted. Spatial resolution is FWHM = 0.1 arcsec, and angular extent is 12×12 arcsec^2. Indicated objects are at small angular separations to the QSO. Object +00004+00019 is a galaxy of angular separation 1.9 arcsec and apparent magnitude $AB(7020) = 22.5$, object −00026+00024 is a galaxy of angular separation 3.5 arcsec and apparent magnitude $AB(7020) = 24.5$, and object −00023+00043 is a galaxy of angular separation 4.9 arcsec and apparent magnitude $AB(7020) = 26.1$.

Fig. 4.— Spatially- and spectrally-resolved image of Hα emission line of WHT ISIS spectrum of galaxy −00089+00020 together with point indicating velocity and impact parameter difference between galaxy and absorption system. Spectral resolution is FWHM = 1.07 Å (or FWHM = 42 km s^{-1}), and spatial resolution is FWHM = 1.69 arcsec (or FWHM = 3.01 h^{-1} kpc). Following Barcons, Lanzetta, & Webb (1995), the projected velocity v and impact parameter ρ are corrected to the line joining the center of the galaxy to the QSO line of sight by assuming circular motion of a flat disk. Contours are equally spaced, at arbitrary levels of intensity.

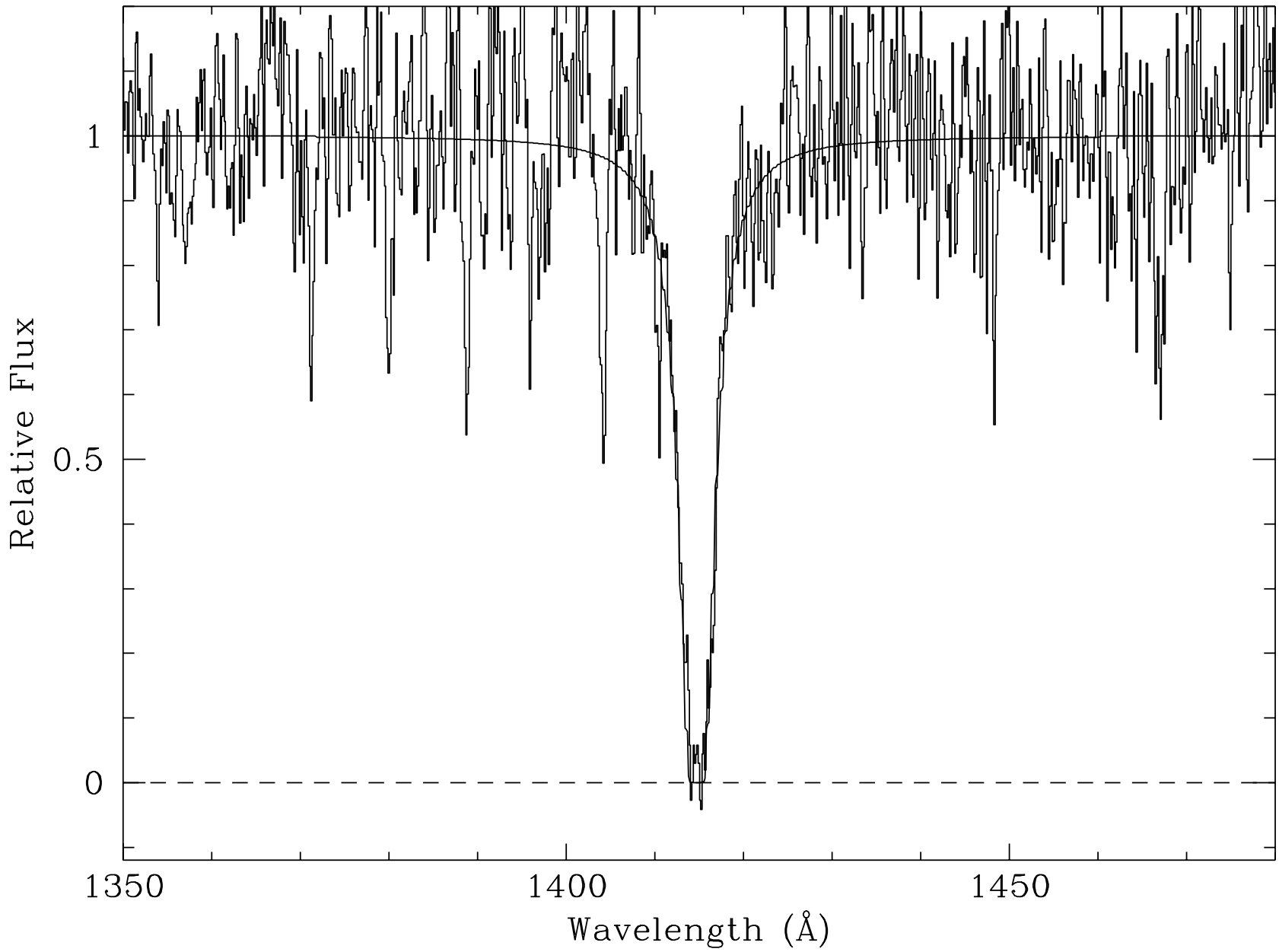
Relative Flux
1
0.5
0
1350
1400
1450
Wavelength (Å)


This figure "damp016.fig2.jpeg" is available in "jpeg" format from:
http://arXiv.org/ps/astro-ph/9707157v1


This figure "damp016.fig3.jpeg" is available in "jpeg" format from:
http://arXiv.org/ps/astro-ph/9707157v1

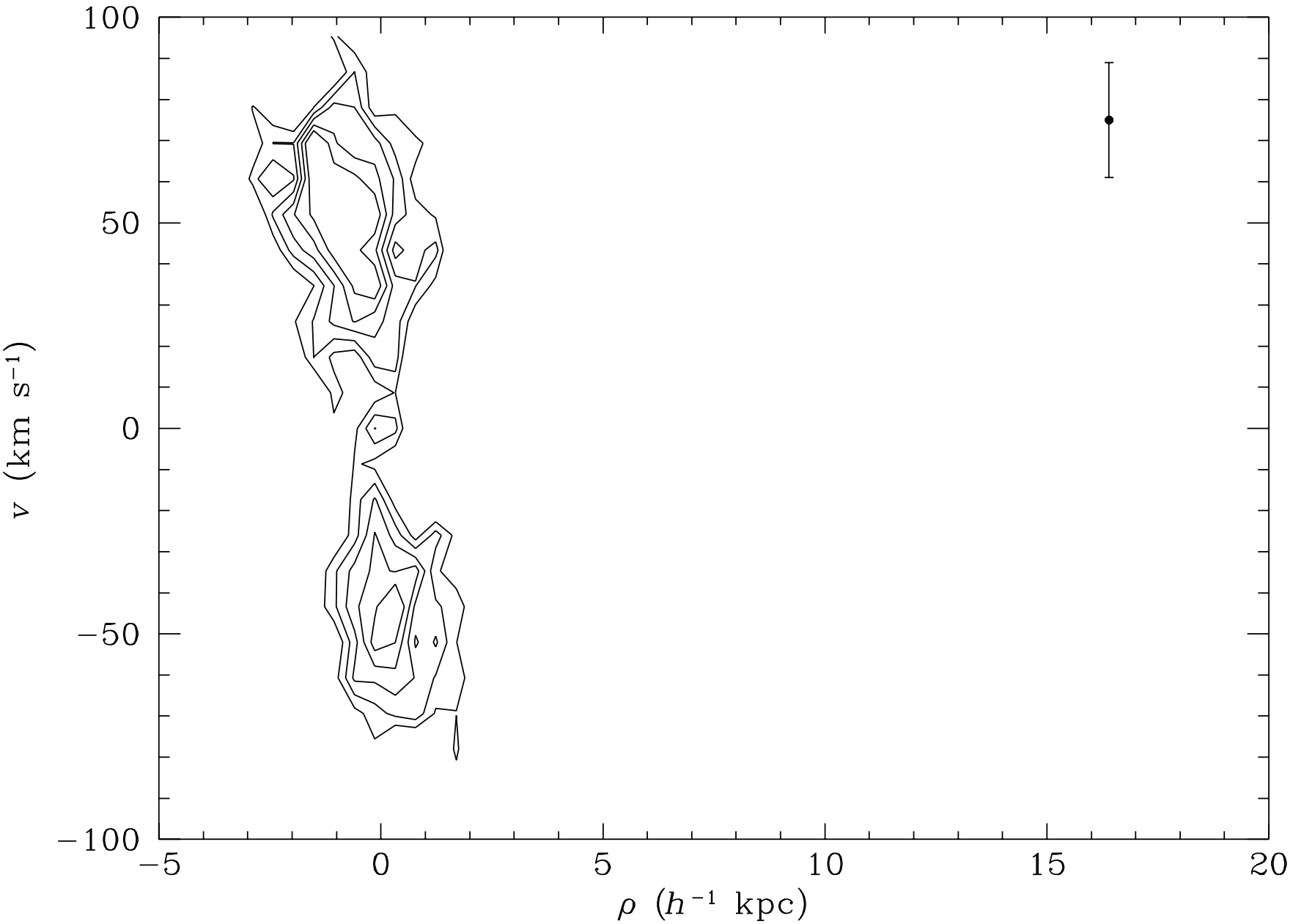
100
50
0
−50
−100
−5
0
5
10
15
20
v (km s−1)
ρ (h−1 kpc)